0026-895X/05/6703-681–694
MOLECULAR PHARMACOLOGY
Vol. 67, No. 3
7278/1194977
Mol Pharmacol 67:681–694, 2005
Printed in U.S.A.

Constitutive Expression of Peroxisome Proliferator-Activated Receptor α-Regulated Genes in Dwarf Mice

Anja J. Stauber,[1] Holly Brown-Borg, Jie Liu, Michael P. Waalkes, Ashley Laughter, Rebecca A. Staben, Jaqueline C. Coley, Cynthia Swanson, Kenneth A. Voss, John J. Kopchick, and J. Christopher Corton

CIIT Centers for Health Research, Research Triangle Park, North Carolina (A.J.S., A.L., R.A.S., J.C.C., C.S.); Department of Pharmacology, Physiology, and Therapeutics, University of North Dakota School of Medicine, Grand Forks, North Dakota (H.B.B.); National Cancer Institute and National Institute of Environmental Health Sciences, Research Triangle Park, North Carolina (J.L., M.P.W.), Toxicology and Mycotoxin Research Unit, Agricultural Research Service, United States Department of Agriculture, Athens, Georgia (K.A.V.), Department of Biomedical Sciences, College of Osteopathic Medicine and Edison Biotechnology Institute, Ohio University, Athens, Ohio (J.J.K.), and ToxicoGenomics, Chapel Hill, North Carolina (J.C.C.)

Received September 15, 2004; accepted November 29, 2004

ABSTRACT

Defects in growth hormone secretion or signaling in mice are associated with decreased body weights (dwarfism), increased longevity, increased resistance to stress, and decreases in factors that contribute to cardiovascular disease and cancer. Peroxisome proliferators (PP) alter a subset of these changes in wild-type mice through activation of the nuclear receptor family member PP-activated receptor α (PPARα). We tested the hypothesis that an overlap in the transcriptional programs between untreated dwarf mice and PP-treated wild-type mice underlies these similarities. Using transcript profiling, we observed a statistically significant overlap in the expression of genes differentially regulated in control Snell dwarf mice (Pit-1^{dw}) compared with phenotypically normal heterozygote (+/*dw*) control mice and those altered by the PP 4-chloro-6-(2,3-xylidino)-2-pyrimidinyl)thioacetic acid (WY-14,643) in +/*dw* mice. The genes included those involved in β- and ω-oxidation of fatty acids (*Acox1*, *Cyp4a10*, *Cyp4a14*) and those involved in stress responses (the chaperonin, T-complex protein1ϵ) and cardiovascular disease (fibrinogen). The levels of some of these gene products were also altered in other dwarf mouse models, including Ames, Little, and growth hormone receptor-null mice. The constitutive increases in PPARα-regulated genes may be partly caused by increased expression of PPARα mRNA and protein as observed in the livers of control Snell dwarf mice. These results indicate that some of the beneficial effects associated with the dwarf phenotype may be caused by constitutive activation of PPARα and regulated genes.

The peroxisome proliferator-activated receptors (PPAR) are members of the nuclear receptor superfamily and are activated by a structurally diverse group of compounds. Many of these compounds increase the size and number of peroxisomes and are thus called peroxisome proliferators (PP). The three PPAR subtypes (α, β/δ, γ) have unique tissue distributions and ligand-specificities. In rodents, PP elicit a predictable course of adaptive responses in the liver, including peroxisome proliferation, induction of lipid-metabolizing genes, and hepatomegaly (Corton et al., 2000). There is overwhelming evidence that PPARα mediates most if not all of these effects in the rodent liver (Lee et al., 1995; Klaunig et al., 2003).

Growth hormone plays an essential role in maintaining cellular and tissue homeostasis. Many PP-regulated genes are under control of growth hormone. Hypophysectomization of female rats enhanced expression of PP-inducible proteins that was reversed by growth hormone infusion (Sugiyama et al., 1994). STAT5b, a growth hormone-inducible transcription factor, inhibited the ability of PPARα to activate PPARα-dependent reporter gene transcription by endogenous or xenobiotic PP in vitro (Zhou and Waxman, 1999a,b). STAT5b-null mice expressed higher levels of some PPARα-regulated gene products involved in lipid metabolism (Zhou et al., 2002).

[1] Current address: Eli Lilly and Company, Greenfield, IN 46140.

Article, publication date, and citation information can be found at http://molpharm.aspetjournals.org.
doi:10.1124/mol.104.007278.

ABBREVIATIONS: PPAR, peroxisome proliferator-activated receptor; PP, peroxisome proliferator; STAT, signal transducer and activator of transcription; WY-14,643, 4-chloro-6-(2,3-xylidino)-2-pyrimidinyl)thioacetic acid; PCR, polymerase chain reaction; RT, reverse transcription; ACO, acyl-CoA oxidase; ANOVA, analysis of variance; APP, acute phase proteins; CR, caloric restriction; CTE, cytosolic thioesterase; GHR, growth hormone receptor; MTE, mitochondrial thioesterase.

These studies provide evidence that growth hormone negatively regulates PPARα in the intact animal through activation of STAT5b.

Strains of dwarf mice have lower circulating levels of growth hormone or defects in growth hormone signaling (Tatar et al., 2003). Snell dwarf mice carry a mutation in the *Pit1* gene (*Pit1*^{dw}) required for development of pituitary cell bodies, which produce growth hormone, prolactin, and thyrotropin. The levels of these hormones are virtually undetectable in these mice. Ames dwarf mice are homozygous for the *df* mutation on the *Prophet of Pit-1* gene (*Prop1*^{df}), a transcription factor controlling expression of *Pit1*. Ames mice have very low levels of circulating growth hormone, prolactin, and thyrotropin. "Little" mice carry a mutation in the growth hormone-releasing hormone receptor (*Ghrhr*) gene and mice homozygous for the *Ghrhr*^{lit} mutation cannot respond to hypothalamic growth hormone-releasing hormone. Little mice have ~5% of normal levels of circulating growth hormone. Inactivation of the growth hormone receptor/binding protein (*Ghr*) by homologous recombination results in a dwarf mouse unable to respond to growth hormone (Zhou et al., 1997). Dwarf mice live significantly longer than their heterozygous littermates maintained under the same conditions (Tatar et al., 2003).

Dwarf mice share phenotypic similarities with PP-treated rodent models. Compared with their heterozygote counterparts, Ames dwarf mice had decreased circulating cholesterol, triglycerides (H. Brown-Borg, unpublished observations), insulin and glucose levels (Borg et al., 1995), whereas growth hormone increased triglyceride and cholesterol levels in wild-type mice (Marmary et al., 1999). PPARα agonists have been used clinically for many years to lower cholesterol and triglyceride levels in patients at risk of coronary heart disease (Corton et al., 2000). Snell dwarf mice had decreased incidences and severities of dimethyl-benzanthracene-induced skin papillomas (Bielschowsky and Bielschowsky, 1961) and sarcoma 180 (Rennels et al., 1965). Ames dwarf mice had decreased numbers and severity grade of spontaneous lung adenocarcinomas (Ikeno et al., 2003), and the Little dwarf mutation suppressed spontaneous liver tumors in the susceptible C3H/HeJ strain (Bugni et al., 2001). In contrast to the well known effects of strong PP on induction of liver cancer (Klaunig et al., 2003), PPARα agonists suppressed certain types of diethyl nitrosamine-induced preneoplastic foci in the rat liver (Cattley and Popp, 1989) as well as skin cancer in mice (Thuillier et al., 2000). PPARα-null mice had a higher incidence of spontaneous hepatocellular adenomas and carcinomas than wild-type mice (Howroyd et al., 2004). Snell dwarf mouse fibroblasts exhibited increased resistance to diverse physical and chemical stressors (Murakami et al., 2003). Likewise, either pretreatment with PPARα agonists in wild-type mice or an intact PPARα gene itself (compared with PPARα-null mice) protected the livers of mice from chemical or physical stress (Mehendale, 2000; Anderson et al., 2002, 2004). One explanation for this phenotypic overlap is that dwarf mice have an increased level of PPARα-regulated gene expression. Although there is clear evidence that STAT5b-null mice express higher levels of PPARα-regulated gene products (Zhou et al., 2002), the effect of mutations in other genes that control growth hormone secretion and signaling on PPARα-regulated gene expression is not known.

We posed the hypothesis that the overlap in the phenotypic characteristics of PP-treated rodents and dwarf mice has at its basis an overlap in the transcriptional programs regulated by PPARα. We tested this hypothesis by examining transcript profiles in the livers of control and PP-treated wild-type and Snell dwarf mice. Our analysis of a number of transcriptional and post-transcriptional targets demonstrated that the overlap includes PPARα-dependent genes with functions in lipid metabolism, stress responses, and cardiovascular disease.

Materials and Methods

Animal Treatments. This study was conducted under federal guidelines for the use and care of laboratory animals and was approved by the Institutional Animal Care and Use Committees for CIIT Centers for Health Research. Male mice were used throughout these studies. Nine-week-old DW/J-Pit1$^{dw/dw}$ln/ln homozygous (*dw*/*dw*) Snell dwarf, DW/J-Pit1$^{+/dw}$ln/ln heterozygous (+/*dw*), C57BL/6J-Ghrhr^{lit} homozygous (*lit*/*lit*) Little dwarf or heterozygous (+/*lit*) mice were purchased from The Jackson Laboratory (Bar Harbor, ME). Wild-type and PPARα-null mice on a SV129 background, ~12 weeks of age, were from a colony established at CIIT. Control and treated mice were provided with NIH-07 rodent chow (Ziegler Brothers, Gardner, PA) and deionized filtered water ad libitum. Lighting was on a 12-h light/dark cycle. Snell dwarf and heterozygous mice were given a single gavage dose of WY-14,643 (ChemSyn Science Laboratories, Lenexa, KS) at a concentration of 50 mg/kg body weight in methylcellulose vehicle (0.1%) and sacrificed 12 h later. Snell, Little mice and their heterozygous control mice were given gavage doses (50 mg/kg body weight) each day for 3 days with sacrifice 24 h after the last dose. Control mice were dosed with methylcellulose (0.1%) vehicle alone. In separate experiments, wild-type and PPARα-null mice were fed a control diet or a diet containing WY-14,643 in the diet (500 ppm) for 1 week. At the designated time after treatment (12 h, 72 h, or 1 week), mice were deeply anesthetized by pentobarbital injection and killed by exsanguination. The livers were removed, rinsed with isotonic saline, snap-frozen in liquid nitrogen, and stored at −70°C until analysis.

Ames dwarf (Prop1^{df}) mice, ~16 weeks of age, and GHR-null mice, ~12 to 16 weeks of age and corresponding groups of age-matched heterozygote (+/*df*) or wild-type mice were maintained at the University of North Dakota (Brown-Borg and Rakoczy, 2000) or Ohio University (Zhou et al., 1997) vivarium facilities. All procedures involving animals were reviewed and approved by the appropriate Institutional Animal Care and Use Committees.

Analysis of Gene Expression by Gene Arrays. Because we were initially interested in effects of dwarf mutations on the ability of PPARα to regulate endpoints associated with liver cancer (Styles et al., 1990), we used the Atlas 1.2 Cancer arrays (BD Biosciences Clontech, Palo Alto, CA) containing 1178 genes with direct or indirect involvement in cancer. Total RNA was isolated by modification of guanidium isothiocyanate method using RNA Stat60 according to the manufacturer's instructions (Tel-Test, Friendswood, TX). ^{32}P-labeled first-strand cDNA was generated by reverse-transcribing poly A$^+$ RNA in the presence of oligo-dT primers. ^{32}P-labeled cDNA was purified using ProbeQuant G-50 Micro Columns (Amersham Biosciences, Piscataway, NJ). Membranes were prehybridized with salmon testes DNA to block nonspecific binding of probe to the membrane. Labeled probes were denatured and incubated with C_ot-1 DNA to block repetitive sequences and subsequently neutralized before adding to the membrane. Labeled probe from each of 12 samples (three mice in each of four groups) representing approximately 2 to 5 $\times$ 10^6 cpm was incubated with a separate but identical array overnight at 68°C. Membranes were heat-sealed in Seal-A-Meal bags and exposed to PhosphorImager autoradiography cassettes for 24 h. Macroarray imaging was performed using the

Molecular Imaging System SI (Bio-Rad, Hercules, CA). Macroarray data analysis was performed using Atlas Image 1.5 software (BD Biosciences Clontech) to determine levels of alterations in gene expression. Local background-subtracted spot intensities (Int) were $\log_2$ transformed. The transformed data were then fitted to this following ANOVA-type model: $Y_{ijk} = \log_2 (Int_{ijk}) = \beta_{ij} (\xi_k) + \delta_{ik} + \Sigma_{ijk}$, where i represents the ith strain/treatment, j represents the jth replicate of a strain/treatment, and k represents the kth gene on the array. In the initial stage, trend effects (ξ_k) are removed by local regression (Kepler et al., 2002), which assumes that the expression of most genes is not changed from treatment to treatment. Genes with low "between-treatment variation" (i.e., variance of the gene across all replicates of all treatments) compared with the "within-treatment variation" (i.e., variance of the replicates of a single treatment) are selected iteratively to create a "not changed" population (i.e., high "within-treatment variation" genes). It is assumed that the "between-treatment effect" for genes in this population is approximately zero. The entire population is then normalized based on this selected subset and the overall treatment effect (δ_{ik}) is calculated. The entire modeling process repeats (in cyclical fashion) until a stable, recurring set of "not changed" genes is obtained. For this ANOVA-type model, the interaction term ($\beta_{ij} (\xi_k)$) considers the "array effect" and "gene effect" to be related; thus, it is nonparametric. The threshold for significance was set at $p < 0.005$, and genes that exhibited a $\geq$1.5-fold or ≤ -1.5-fold were reported as a $\log_2$ fold-change relative to the control. Regulated genes were visualized using CLUSTER and TreeView (Eisen et al., 1998). Spearman rank correlation test of the regulated genes was performed using SAS (ver. 6.12; SAS Institute, Research Triangle Park, NC).

Real-Time RT-PCR Analysis. Expression levels of selected genes were quantified using real-time RT-PCR analysis. In brief, total RNA was extracted as described above, purified with RNeasy column and on-column DNase I digestion (QIAGEN, Valencia, CA). Purified total RNA was reverse-transcribed with MuLV reverse transcriptase and oligo-dT primers. The forward and reverse primers (Table 1) were designed using Primer Express software, v2.0 (Applied Biosystems, Foster City, CA). The SYBR green PCR master mix (Applied Biosystems) was used for real-time PCR analysis. The dissociation curve (melting curve) for each gene was performed to verify the quality of the primers. The standard curve for each gene was performed to quantify the gene expression. The expressions of genes were first normalized with 18 S ribosomal RNA gene of the same sample, and then the relative differences between control and treatment groups were calculated and expressed as relative increases setting the control as 100%.

Analysis of Palmitoyl-CoA Oxidase Activity. Analysis of palmitoyl-CoA oxidase activity was determined using the procedures in Sausen et al. (1995). Liver from the left lobe was used to prepare 20% homogenates in 50 mM Tris-HCl and 154 mM KCl, pH 7.2. Homogenates were prepared on the day of enzyme assays by centrifugation at 2500*g* for 10 min. Palmitoyl-CoA oxidase activity was assayed by measurement of hydrogen peroxide production in the presence of 25 μM palmitoyl-CoA. Enzyme activity was normalized per gram of protein.

Western Analysis. Liver lysates were prepared in 250 mM sucrose, 10 mM Tris-HCl, pH 7.4, and 1 mM EDTA with protease inhibitors (0.2 mM phenylmethylsulfonyl fluoride, 0.1% aprotinin, 1 μg/ml pepstatin, and 1 μg/ml leupeptin). Fifty micrograms of whole-cell lysate was subjected to 12% SDS-polyacrylamide gel electrophoresis followed by transfer to nitrocellulose membranes. Immunoblots were developed using primary antibodies against acyl-CoA oxidase (ACO) (a gift from Dr. S. Alexson, Huddinge University Hospital, Huddinge, Sweden), MFP-I, MFP-II, and thiolase (gifts from Dr. T. Hashimoto, Japan), Cyp4a (BD Gentest, Waltham, MA), PPARα (Affinity Bioreagents, Inc., Golden, CO), T-complex protein1ϵ, and other chaperones and chaperonins (Stress Gen, Victoria, BC, Canada), and α1-antitrypsin and fibrinogen (Affinity Biologicals, South Bend, IN) followed by appropriate secondary antibodies conjugated with horseradish peroxidase (Santa Cruz Biotechnology, Santa Cruz, CA) in the presence of chemiluminescent substrate ECL (Amersham Biosciences, Piscataway, NJ). Cyp4a antibody probably recognizes multiple members of the Cyp4a family (Cyp4a10, Cyp4a12, Cyp4a14). MFP-I probably recognizes multiple forms of the MFP-I complex, including protein products encoded by *Dci*, *Ech1*, and *Ehhadh*. MFP-II was raised against the product of the gene *Hsd17b4*. Blots were quantitated densitometrically (BioRad Imaging Densitometer and Molecular Analyst software) after exposure of the membrane to X-ray film.

TABLE 1
List of primers used in the RT-PCR studies

Gene	GenBank Accession Number	Forward Primer	Reverse Primer
18S	X56974	CGAACGTCTGCCCTATCAACTT	CCGGAATCGAACCCTGATT
Acox1	AF006688	GGGAGTGCTACGGGTTACATG	CCGATATCCCCAACAGTGATG
Cct3	L20509	CCATGCACAGAACCAGCAGTT	GGCTGCCCCTCAACCTAATC
Cct5	NM_007637	CCGTGACAACCGTGTTGTGTAT	CTTGTCTGCCTCTTGGCTGACT
Cct7	Z31399	TGGCCACCCAGTACTTTGCT	GAGCCTCCACAAGCCATCAT
Ccnd1	M64403	GGGCACCTGGATTGTTCT	CACCGGAGACTCAGAGCA
Cte1	NM_012006	GGAAGGAGAAGCCCCAGATC	CTGCACAGCGGGAAGTAAGG
Cyp4a10	AB018421	CCAGGAACTGCATTGGGAAA	GACCCTGGTAGGATCTGGCA
Cyp4a14	Y11638	GGTGAGGCTGATTGAGTCTTGAG	CTCCAGATTGATCCAGGATGGA
Dci	NM_010023	CCTCAGCTTGGAGTGTCTCACA	GACACCTCGGATGCTCTTGTC
Ech1	NM_016772	GACTGCCGGGCTGTTGTAGT	GTTCGGAGGCCATGTCCAT
Ehhadh	NM_023737	GTTGGCTTCCCGGAAGTGAT	CTCCAACGACCCTGGGTAGA
Fabp4	M20497	AGTCACATGGTCAGGGCATCTT	AACCTTCGAGGAGGAGCTGTCT
Fgb	NM_181849	GCACTGTCAGCTGCAACATTC	GGATGTCTCACCTCCCTTCCT
Hsp25	U03560	GAAGAAAGGCAGGACGAACATG	CACCTGGAGGGAGCGTGTAT
Hsp32	M33203	CCTCACTGGCAGGAAATCATC	CCTCGTGGAGACGCTTTACATA
Hsp40	U40992	GGTGTGCACTCAGACGAAAGC	CCAGGCTAGCTCCAAAGAACA
Hsp60	X55023	TCAGTCCATTGTCCCTGCTCTT	GTGCTTAGAGCTTCTCCGTCAAC
Hsp70	M35021	GGACAAGCAAGCATTCCACA	CTCAAGAGAGGCGGGATAAGG
Hsp86	X16857	CGGACGCTCTGGATAAAATCC	TCCTTCCCCGAGTCCAGTTT
Hsp105	D67016	ATCTCTGGTCTGGAACCACGA	TCAGGAAGGTGAGCACTTTGG
Igf1	X04480	TTGCTTCCGGAGCTGTGATC	AGAGCGGGCTGCTTTTGTAG
Igfbp1	X81579	TGGACAGCTTCCACCTGATG	TGATGGCGTTCCACAGGAT
Mte1	NM_134188	GGAAGGAGAAGCCCCAGATC	CTGCACAGCGGGAAGTAAGG
Pex11a	AF093669	TCCTGGACACCGTGAAGAACT	CGCCGAGATTGGACTTGTAGA
Ppara	AI323000	AAGCCATCTTCACGATGCTG	TCAGAGGTCCCTGAACAGTG

Statistical Analysis of Data. Means and S.E.M. (n = 3–4) for RT-PCR data were calculated by the Students' t test. The level of significance was set at $p \leq 0.05$. The expression ratios between WY-14,643-treatment and control mice and between dwarf mice and heterozygote mice were used for comparisons. For Western data, a two-way ANOVA was used to determine statistical significance ($p \leq 0.05$). Students' t tests were used for comparisons within genotype when significant interactions were detected between genotype and treatment. Spearman rank correlation test was performed using SAS.

Results

The *pit-1^{dw}* Mutation Results in Constitutive Increases in a Subset of WY-14,643-Responsive Genes. We used transcript profiling to gain insight into the underlying gene expression patterns that may explain phenotypic similarities between dwarf mice and PP-treated heterozygote mice. Heterozygous (+/*dw*) and homozygous (*dw*/*dw*) Snell dwarf mice were treated with the PP WY-14,643 or methylcellulose carrier and sacrificed 12 h later. The livers were examined for gene expression using the Atlas mouse cancer 1.2 arrays containing 1178 genes. Genes with a p value $\leq$0.005 and $\geq$1.5-fold or ≤ -1.5-fold were reported as a $\log_2$ fold-change relative to the respective control genes. Regulated genes were visualized using CLUSTER and TreeView programs (Eisen et al., 1998) using two-dimensional clustering. Figure 1A shows the 111 genes with significant changes in one or more groups. The regulated genes were divided into groups (A–H) based on expression behavior differences. Although the Atlas mouse cancer arrays do not contain typical markers of PPARα activation such as genes involved in fatty acid β-oxidation, the genes regulated by WY-14,643 in the +/*dw* mice versus control +/*dw* mice (Fig. 1A, groups B–D, F, and G) included genes or their products regulated by PP in other studies. These genes were cathepsin B (Conway et al., 1989), adipose differentiation-related protein (Liu et al., 2003), as well as PPARα itself (Sterchele et al., 1996) (Table 2). WY-14,643 exposure in +/*dw* mice also led to increased expression of chaperones (Hsp86 and Hsp84) and chaperonin genes [chaperonin subunits 4 (δ), 6a (ζ), 6b (ζ), 7 (η)]. We showed in recent studies that PP exposure increases expression of a large number of genes in wild-type mice that maintain the health of the proteome, including Hsp86 and chaperonin subunits (Anderson et al., 2004).

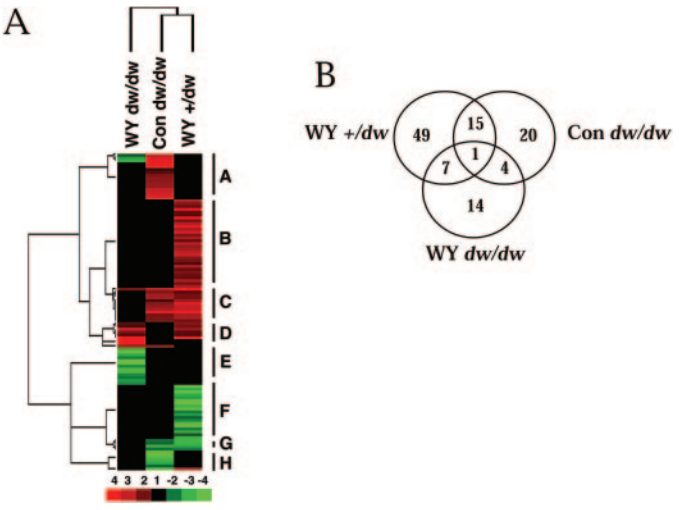

Fig. 1. Altered gene expression in *dw*/*dw* Snell dwarf mice before and after WY-14,643 treatment. Heterozygous (+/*dw*) and homozygous (*dw*/*dw*) dwarf mice were administered a single gavage dose (50 mg/kg) of WY-14,643 in methylcellulose or methylcellulose alone and sacrificed after 12 h. Gene expression was determined using Atlas Cancer 1.2 macroarrays (BD Biosciences Clontech) as described under *Materials and Methods*. Genes whose expression was significantly ($p < 0.005$) different between two or more groups and exhibited a $\geq$1.5-fold or ≤ -1.5-fold change were reported as a $\log_2$ fold-change relative to the corresponding control. Significant genes were clustered and visualized using CLUSTER and TreeView. A, two-dimensional cluster diagram of similarly regulated genes showing groups A–H (described in further detail in the text). The numbers on the scale are in -fold change. "WY *dw*/*dw*" show the changes in WY-14,643 treated *dw*/*dw* mice normalized to control *dw*/*dw* mice. "Con *dw*/*dw*" show the changes in control *dw*/*dw* mice normalized to control +/*dw* mice. "WY +/*dw*" show the changes in WY-14,643 treated +/*dw* mice normalized to control +/*dw* mice. B, Venn diagram showing the overlap in the genes regulated by *Pit1^{dw}* or WY-14,643 in the +/*dw* or *dw*/*dw* strains.

The *dw* mutation itself resulted in the altered regulation of a total of 41 genes found within groups A, C, G and H (Fig. 1A). Using GenBank numbers as unique identifiers, we compared our list of genes with the genes identified as different in 6-month-old *dw*/*dw* mice compared with wild-type control mice using a similar array platform (Dozmorov et al., 2002). Only four of the genes identified in the previous study (insulin receptor, interleukin 15, Cyp1a1, and insulin-like binding protein 1) were altered in one of the three comparisons in our study. None of these genes was significantly altered in the control *dw*/*dw* versus control +/*dw* mice in our study; however, insulin-like binding protein 1 (*Igf1bp1*) was up-regulated in control *dw*/*dw* versus control +/*dw* mice (~2-fold; $p = 0.034$) but did not pass the statistical cut-off. *Igf1bp1* was found by RT-PCR to be induced in control *dw*/*dw* mice (Table 3). The fact that there was no overlap in the two studies could be attributable to differences in animal husbandry and age of mice (9 weeks versus 6 months.).

Hierarchical clustering of the compared groups showed that the control *dw*/*dw* pattern was more similar to that of the WY-14,643-treated +/*dw* pattern than that of the pattern of WY-14,643-treated *dw*/*dw* mice (Fig. 1A). We used Spearman correlation to determine the statistical significance of similarities between groups. The control *dw*/*dw* pattern was more similar to WY-14,643 +/*dw* pattern (0.216, $p = 0.023$) than the WY-14,643 *dw*/*dw* pattern (-0.013; $p = 0.892$). This similarity was driven primarily by 16 of 40 genes (40%) similarly regulated in control *dw*/*dw* and WY-14,643-treated +/*dw* mice. These included 12 up-regulated (group C) and 4 down-regulated (group G) genes (Fig. 1B). The genes included down-regulation of receptors for interleukin-1 and interferon γ (Fig. 1, group G) predicted to decrease responsiveness to these inflammatory mediators. These data indicate that control *dw*/*dw* mice constitutively express genes that are also regulated by WY-14,643 in +/*dw* mice.

The WY-14,643 +/*dw* and WY-14,643 *dw*/*dw* patterns exhibited similarity that approached significance (0.179; $p = 0.06$). WY-14,643 treatment in *dw*/*dw* mice did little to further alter the expression of most of the overlapping genes regulated in *dw*/*dw* mice. However, two genes up-regulated in control *dw*/*dw* mice (epoxide hydrolase 1, microsomal and RAN) were further up-regulated by WY-14,643, whereas three genes up-regulated in control *dw*/*dw* mice [angiotensin II receptor, type 2; protein tyrosine phosphatase, receptor type, M; cell division cycle 2 homolog (*Schizosaccharomyces*

TABLE 2

Gene expression altered by the Pit1^{dw} mutation or exposure to WY-14,643

Gene classes were determined by hierarchical clustering (Fig. 1A). Gene coordinates, NCBI numbers, and names are according to BD Biosciences Clontech.

Class	Coordinate	NCBI Number	Gene Name	FC, WY dw/dw	*P* Value WY dw/dw	FC CON dw/dw	*P* Value CON dw/dw	FC WY +/dw	*P* Value WY +/dw
A	F05g	L19622	tissue inhibitor of metalloproteinase 3			4.69	0.00011		
	F04 h	M64085	serine (or cysteine) proteinase inhibitor, clade A, member 3G			3.83	0.00027		
	A05n	M58633	cell division cycle 2 homolog (*S. pombe*)-like 1	−2.94	0.00087	3.76	0.00453		
	A08j	Y00051	neural cell adhesion molecule 1			3.48	0.00420		
	F06g	X58287	protein tyrosine phosphatase, receptor type, M	−2.51	0.00149	3.46	0.00185		
	C06e	X78987	epidermal growth factor receptor			3.38	0.00068		
	E11a	S53270	cell line NK14 derived transforming oncogene			3.07	0.00083		
	C06m	X78568	FMS-like tyrosine kinase 1			3.03	0.00332		
	C10 h	L32840	angiotensin II receptor, type 2	−1.54	0.00033	2.79	0.00003		
	B10g	X58251	procollagen, type I, α2			2.36	0.00061		
	F05k	M36033	protein tyrosine phosphatase, receptor type, A			2.26	0.00398		
	C07c	AF002701	glial cell line derived neurotrophic factor family receptor α 2			2.23	0.00317		
	F07g	AB011678	doublecortin			2.20	0.00087		
	C05l	Y12879	D6 β-chemokine receptor			2.04	0.00499		
	E06j	AF099067	NIMA (never in mitosis gene a)-related expressed kinase 4			1.65	0.00155		
	A10a	U83190	zonadhesin			1.50	0.00013		
B	A14i	M93275	adipose differentiation related protein					4.76	0.00074
	B13j	Z31557	chaperonin subunit 6a (ζ)					3.70	0.00040
	D04 h	M74181	macrophage stimulating 1 (hepatocyte growth factor-like)					3.67	0.00240
	A05b	L49507	cyclin G1					3.35	0.00127
	A04b	U57634	nuclear factor I/B					3.17	0.00177
	C04j	X58196	H19 fetal liver mRNA					2.89	0.00067
	B07b	U62295	cytochrome P450, family 2, subfamily j, polypeptide 6					2.87	0.00001
	D10 h	D14716	adenylate cyclase activating polypeptide 1					2.75	0.00188
	E09i	D28117	protein phosphatase 1A, magnesium dependent, α isoform					2.66	0.00262
	F01l	U77083	alanyl (membrane) aminopeptidase					2.64	0.00386
	E01j	X85999	interleukin 1 receptor accessory protein					2.60	0.00330
	A02f	AB000096	GATA binding protein 2					2.52	0.00036
	B12d	AF090317	cytochrome P450, family 8, subfamily b, polypeptide 1					2.50	0.00311
	B13 h	Z31554	chaperonin subunit 4 (delta)					2.48	0.00020
	D10a	U14332	interleukin 15					2.48	0.00434
	B12k	U85511	expressed in nonmetastatic cells 1, protein					2.31	0.00001
	B11g	U93309	discs, large homolog 1 (Drosophila)					2.16	0.00147
	B06 h	AF055664	DnaJ (Hsp40) homolog, subfamily A, member 1					2.10	0.00286
	C03e	AF041054	BCL2/adenovirus E1B 19kDa-interacting protein 1, NIP3					2.06	0.00081
	B08n	M63802	gap junction membrane channel protein β 1					2.01	0.00056
	B03 h	X57638	peroxisome proliferator-activated receptor α					1.98	0.00076
	E08j	U22445	thymoma viral proto-oncogene 2					1.97	0.00159
	B10l	L02918	procollagen, type V, α 2					1.97	0.00130
	D11n	AF033585	frizzled homolog 9 (*Drosophila melanogaster*)					1.86	0.00331
	D05c	X81579	insulin-like growth factor binding protein 1					1.83	0.00435
	E11k	X57277	RAS-related C3 botulinum substrate 1					1.80	0.00041
	B07 h	U48420	glutathione S-transferase, θ 2					1.78	0.00051
	B09d	U72680	FXYD domain-containing ion transport regulator 5					1.78	0.00482
	E10l	U89694	protein tyrosine phosphatase, nonreceptor type substrate 1					1.75	0.00233
	A14m	AF110802	interleukin 18 binding protein					1.69	0.00442
	B02i	Z50013	Harvey rat sarcoma virus oncogene 1					1.66	0.00116

TABLE 2 (continued)

Gene expression altered by the Pit1^{dw} mutation or exposure to WY-14,643

Gene classes were determined by hierarchical clustering (Fig. 1A). Gene coordinates, NCBI numbers, and names are according to BD Biosciences Clontech.

Class	Coordinate	NCBI Number	Gene Name	FC, WY dw/dw	*P* Value WY dw/dw	FC CON dw/dw	*P* Value CON dw/dw	FC WY +/dw	*P* Value WY +/dw
C	E11m	L32751	RAN, member RAS oncogene family	1.88	0.00093	2.73	0.00078	6.54	0.00011
	E11i	Y00094	RAB1, member RAS oncogene family			3.50	0.00176	4.77	0.00205
	E11l	L20294	SAR1a gene homolog (*Saccharomyces cerevisiae*)			2.13	0.00162	3.54	0.00000
	A06k	L16846	B-cell translocation gene 1, anti-proliferative			2.50	0.00208	3.04	0.00239
	F02m	S69034	cathepsin B			2.34	0.00313	3.00	0.00208
	E07k	X61940	dual specificity phosphatase 1			2.03	0.00095	2.67	0.00044
	B13k	Z50192	chaperonin subunit 6b (ζ)			1.98	0.00068	2.57	0.00050
	A13 h	J05287	lysosomal membrane glycoprotein 2			1.59	0.00031	2.37	0.00250
	D11g	U66203	fibroblast growth factor 11			1.94	0.00368	1.96	0.00097
	B08k	X61675	gap junction membrane channel protein α 5			2.52	0.00081	1.95	0.00188
	E01 h	AJ001373	integrin β 1 binding protein 1			2.52	0.00065	1.95	0.00131
	E11j	X72966	RAB3A, member RAS oncogene family			2.03	0.00258	1.70	0.00054
D	B13a	M15009	cytochrome P450, family 21, subfamily a, polypeptide 1	21.89	0.00008				
	B06l	M14757	ATP-binding cassette, subfamily B (MDR/TAP), member 1B	5.99	0.00132				
	B14 h	M36830	heat shock protein 1, α	3.78	0.00451			3.34	0.00047
	F06m	M21495	actin, γ, cytoplasmic	3.11	0.00441			2.35	0.00133
	B07c	U89491	epoxide hydrolase 1, microsomal	2.12	0.00237	2.08	0.00025		
	B14g	M18186	heat shock protein 1, β	2.05	0.00175			1.70	0.00135
	F10m	X72091	vitronectin	1.62	0.00439			1.63	0.00201
	E10b	U84411	protein tyrosine phosphatase 4a1	1.59	0.00420			2.11	0.00100
	F10l	M98454	villin	1.56	0.00327			1.93	0.00441
E	B08j	X57971	gap junction membrane channel protein α 4	−5.59	0.00360				
	F06f	Z37988	protein tyrosine phosphatase, receptor type, F	−5.58	0.00027				
	C02n	U59746	Bcl2-like 2	−4.99	0.00333				
	D05g	U60530	MAD homolog 2 (*D. melanogaster*)	−3.29	0.00050				
	D06j	M23503	chemokine (C-C motif) ligand 4	−3.28	0.00030				
	A12k	X79082	Eph receptor A7	−3.27	0.00210				
	B11l	X00479	cytochrome P450, family 1, subfamily a, polypeptide 1	−2.73	0.00471				
	F07f	Z22923	procollagen, type IX, α 2	−2.50	0.00403				
	A06n	U70017	cyclin D binding myb-like transcription factor 1	−2.21	0.00192				
	B10k	AF169387	procollagen, type IV, α 3	−2.16	0.00318				
	D08f	U61969	wingless related MMTV integration site 10a	−2.15	0.00308				
	A03l	L07911	kappa B and Rss recognition component	−2.00	0.00243				
	B09g	AF115383	dystonin	−1.97	0.00012				
F	C05d	Z23143	bone morphogenetic protein receptor, type 1B					−9.91	0.00206
	C05 h	U47035	chemokine (C-C) receptor 2					−8.97	0.00218
	C14l	X80764	tyrosine kinase receptor 1					−6.71	0.00202
	F11d	X66323	X-ray repair complementing defective repair in Chinese hamster cells 5					−5.43	0.00242
	C10n	J05149	insulin receptor					−4.82	0.00384
	E06d	D87115	mitogen activated protein kinase kinase 3					−4.04	0.00424
	A14e	X97818	semaphorin 5B					−3.63	0.00190
	F13f	Y09688	nth (endonuclease III)-like 1 (*E. coli*)					−2.97	0.00047
	C13c	M27150	Fc receptor, IgE, low affinity II, α polypeptide					−2.93	0.00472
	C11n	M23376	CD3 antigen, epsilon polypeptide					−2.89	0.00064
	C11f	X51983	thyroid hormone receptor α					−2.79	0.00405
	D02d	M13926	colony stimulating factor 3 (granulocyte)					−2.77	0.00223
	C06f	L47239	v-erb-b2					−2.45	0.00272
	F07b	AF026489	spectrin β 3					−2.43	0.00098
	A06c	U19597	cyclin-dependent kinase inhibitor 2D (p19, inhibits CDK4)					−2.18	0.00049
	F10b	U52826	syndecan 3					−2.03	0.00029
	C14e	M60909	retinoic acid receptor, α					−1.99	0.00124
	A07c	U43525	proteinase 3					−1.70	0.00308
	C12b	M33158	CD3 antigen, ζ polypeptide					−1.51	0.00358

pombe)-like 1] were down-regulated by WY-14,643, indicating more complex control by the *Pit-1*^{dw} gene and WY-14,643.

Given the overlap in the transcript profiles of control *dw/dw* and WY-14,643 in *+/dw*, we determined the mRNA expression of known PPARα-regulated genes in the livers of *+/dw* and *dw/dw* mice treated with WY-14,643 or carrier for 3 days. We chose a 3-day treatment period to facilitate comparison of mRNA and protein levels described in further detail below. Genes with known roles in fatty acid metabolism were induced by WY-14,643 in *+/dw* mice, as expected. The genes included *Acox1* (acyl-CoA oxidase 1, peroxisomal), *Cte1* (cytoplasmic thioesterase 1), *Cyp4a10*, *Cyp4a14*, *Dci* (dodecenoyl-CoA delta isomerase), *Ech1* (enoyl CoA hydratase 1, *Ehhadh* (enoyl-CoA, hydratase/3-hydroxyacyl CoA dehydrogenase), *Fabp4* (fatty acid binding protein 4), *Mte1* (mitochondrial thioesterase 1), and *Pex11a* (peroxisomal biogenesis factor 11a) (Table 3). A number of these genes were constitutively up-regulated in control *dw/dw* mice compared with control *+/dw* mice including *Acox1*, *Cyp4a10*, *Cyp4a14*, *Dci*, *Ech1*, *Ehhadh*, *Fabp4*, and *Pex11a*; *Acox1*, *Cyp4a10*, *Cyp4a14*, *Ech1*, and *Ehhadh* and *Fabp4* achieved significance. A subset of these genes was further increased in dwarf mice including *Acox1*, *Cyp4a10*, *Cyp4a14*, *Dci*, and *Ehhadh*; *Acox1*, *Cyp4a10*, *Cyp4a14*, *Dci*, and *Ehhadh* became significant. The remaining genes, except for *Fabp4* and *Pex11a*, were increased by WY-14,643 in dwarf mice to about the same extent in dwarf and heterozygote mice.

Genes involved in a number of other functional categories

TABLE 2 (continued)

Gene expression altered by the Pit1^{dw} mutation or exposure to WY-14,643

Gene classes were determined by hierarchical clustering (Fig. 1A). Gene coordinates, NCBI numbers, and names are according to BD Biosciences Clontech.

Class	Coordinate	NCBI Number	Gene Name	FC, WY dw/dw	*P* Value WY dw/dw	FC CON dw/dw	*P* Value CON dw/dw	FC WY +/dw	*P* Value WY +/dw
G	C08n	M20658	interleukin 1 receptor, type I			−1.90	0.00240	−3.12	0.00181
	C01k	S56660	retinoic acid receptor, β			−1.76	0.00243	−3.03	0.00264
	C08m	M28233	interferon γ receptor			−3.08	0.00098	−2.67	0.00349
	F06b	D88187	protein tyrosine phosphatase, receptor type, L			−1.87	0.00010	−2.04	0.00001
H	B12m	M64863	cytochrome P450, family 17, subfamily a, polypeptide 1			−5.51	0.00352		
	B13l	Z31399	chaperonin subunit 7 (η)			−4.06	0.00062	2.46	0.00008
	F13c	U66887	RAD50 homolog (*S. cerevisiae*)			−4.00	0.00068		
	B07f	U87147	flavin containing monooxygenase 3			−3.41	0.00159		
	E13a	X95346	phospholipase C, γ 1			−2.95	0.00046		
	F07c	X53929	decorin			−2.65	0.00175		
	F10d	L07803	thrombospondin 2			−1.77	0.00155		

WY, *dw/dw*: changes in gene expression by WY in *dw/dw* mice compared with control *dw/dw* mice; Con, *dw/dw*: changes in the expression of genes in control *dw/dw* mice compared with control *+/dw* mice; WY, *+/dw*: changes in gene expression by WY in *+/dw* mice compared with control *+/dw* mice.

TABLE 3

Real-time RT-PCR analysis of selected gene expression in response to WY-14,643 in WT and Snell dwarf mice

Data are mean ± S.E.M. of four individual animals.

Gene categories	WT-Con	WT-WY	-Fold Change	Dwarf-Con	Dwarf-WY	-Fold of Con
Lipid Metabolism						
Acox1	100 ± 8	235 ± 25	2.35*	184 ± 24‡	487 ± 47	2.7*†
Cte1	100 ± 8	1020 ± 300	10.2*	128 ± 25	1100 ± 80	11*
Cyp4a10	100 ± 13	1950 ± 400	19.5*	1430 ± 370‡	4360 ± 450	3.0*†
Cyp4a14	100 ± 30	1110 ± 250	11.1*	1960 ± 490‡	2740 ± 560	1.4*†
Dci	100 ± 12	300 ± 50	3.0*	155 ± 36	570 ± 60	3.7*†
Ech1	100 ± 15	285 ± 40	2.9*	190 ± 40‡	390 ± 30	2.2*
Ehhadh	100 ± 8	1240 ± 120	12.4*	200 ± 40‡	2660 ± 350	13.4*†
Fabp4	100 ± 14	240 ± 30	2.4*	160 ± 17‡	160 ± 25	1.0
Mte1	100 ± 9	580 ± 150	5.8*	90 ± 20	780 ± 160	8.0*
Pex11a	100 ± 13	215 ± 30	2.2*	160 ± 30	150 ± 10	0.9
IGF axis						
IgfI	100 ± 10	105 ± 14	1.0	2 ± 0‡	1 ± 0	0.8†
Igfbp1	100 ± 13	86 ± 20	0.9	5850 ± 1650‡	5980 ± 807	1.0†
Chaperones						
Cct3	100 ± 14	150 ± 30	1.5	175 ± 17‡	200 ± 19	1.1
Cct5	100 ± 10	120 ± 20	1.2	172 ± 35‡	200 ± 25	1.2
Cct7	100 ± 10	80 ± 16	0.8	150 ± 35	135 ± 10	0.9
Hsp27	100 ± 15	150 ± 30	1.5	60 ± 20	90 ± 30	1.5
Hsp32	100 ± 12	120 ± 20	1.2	125 ± 12	135 ± 50	1.3
Hsp40	100 ± 10	120 ± 16	1.2	135 ± 10	130 ± 14	1.0
Hsp60	100 ± 13	150 ± 24	1.5	163 ± 28‡	190 ± 30	1.2
Hsp70	100 ± 8	130 ± 20	1.3	220 ± 45‡	160 ± 22	0.8
Hsp86	100 ± 11	110 ± 15	1.1	100 ± 15	104 ± 12	1.0
Hsp105	100 ± 31	70 ± 15	0.7	130 ± 30	100 ± 20	0.8
Miscellaneous						
Ccnd1	100 ± 10	150 ± 40	1.5	60 ± 10‡	54 ± 5	0.9
Fbb	100 ± 4	80 ± 8	0.8	64 ± 10‡	68 ± 4	1.1

* Significantly different from controls $P < 0.05$.
† Significantly different from WT-WY, $P < 0.05$.
‡ Significantly different from WT-Con, $P < 0.05$.

were examined. Insulin signaling pathways were altered in control *dw/dw* mice including dramatic down-regulation of *Igf1* (insulin-like growth factor 1) and up-regulation of *Igfbp1*. WY-14,643 did not alter the expression of these genes. Genes that help maintain the health of the proteome (*Cct3*, *Cct5*, *Hsp60*, *Hsp70*) were up-regulated in control *dw/dw* mice versus control *+/dw* mice. Fibrinogen β-chain (*Fab*) previously shown to be down-regulated by PP (Corton et al., 1998) and cyclin D1 (*Ccnd1*) were down-regulated in *dw/dw* mice. These results demonstrate that control *dw/dw* mice exhibit features of their transcriptional profiles similar to PP-treated heterozygote mice.

We next examined the expression of gene products regulated by PP in a PPARα-dependent manner in the liver. ACO, the first rate-limiting enzyme in the fatty acid β-oxidation pathway, is expressed as an inactive precursor (ACO-A) cleaved to active forms ACO-B and ACO-C. The antibody we used can detect ACO-C, but because expression is weak and sometimes variable, only ACO-A and ACO-B forms are shown in the following experiments. Levels of ACO protein expression were barely detectable in untreated +/*dw* mice (Fig. 2A). WY-14,643 treatment increased ACO-A and ACO-B levels in +/*dw* mice after 3 days of exposure. In the absence of WY-14,643 treatment, *dw/dw* mice express higher levels of ACO-B compared with untreated +/*dw* mice, but the increase was not significant (Fig. 2, A and B). After exposure to WY-14,643, ACO-A but not ACO-B levels were increased in the livers of *dw/dw* mice to the same extent as those in control animals. Palmitoyl-CoA oxidase activity, a measure of ACO activity, was increased in WY-14,643-trreated +/dw mice compared with control +/*dw* mice but did not reach statistical significance in *dw/dw* WY-14,643-treated versus control mice (Fig. 2C).

Cyp4a protein levels were increased in WY-14,643-treated +/*dw* mice compared with control mice (Fig. 2, A and B). The control *dw/dw* mice constitutively express higher levels of Cyp4a protein compared with control treated +/*dw* mice. In *dw/dw* mice, treatment with WY-14,643 did not further increase Cyp4a expression above that observed in the untreated *dw/dw* control mice.

Other gene products regulated by PPARα were also examined, including three proteins involved in peroxisomal fatty acid β-oxidation [multifunctional protein-I (MFP-I), MFP-II, and thiolase] and cytosolic and mitochondrial thioesterases [CTE-1 and MTE-1]. Control *dw/dw* mice did not exhibit statistically significant increases in MFP-I, MFP-II, MTE-I, thiolase, and CTE-I (Fig. 2, D and E). Thus, not all PP-responsive gene products are regulated in a similar manner by the $pit\text{-}1^{dw}$ mutation as seen in the RT-PCR studies. MFP-II and thiolase exhibited significantly greater increases in expression after WY-14,643 exposure in *dw/dw* mice than in +/*dw* mice, indicating that *dw/dw* mice are more responsive to PP induction of these gene products. Although these changes in protein expression are generally consistent with the RT-PCR results, differences may reflect both transcriptional and posttranscriptional control mechanisms by Pit^{dw} and WY-14,643.

To begin to explain the constitutive activation of PPARα-regulated genes, we determined whether PPARα mRNA and protein levels were directly altered in *dw/dw* mice. Messenger RNA levels of PPARα were elevated in control *dw/dw* mice compared with the +/*dw* mice (Fig. 3). In parallel with the PPARα mRNA, PPARα protein levels were increased ~2.3-fold compared with +/*dw* mice. No changes were observed after WY-14,643 exposure in any strain. These results indicate that the increased expression of PPARα gene targets in the livers of untreated Snell dwarf mice may be partly caused by increased expression of PPARα.

Alteration of PPARα-Regulated Gene Products in Other Dwarf Mouse Models. We examined expression of PP-dependent gene products in other types of dwarf mice. In control homozygous Ames mice (*df/df*), ACO-B, and Cyp4a protein expression levels were increased compared with their heterozygote (+/*df*) littermates (Fig. 4A). Other proteins examined above were not grossly affected in the *df/df* mouse strain under these conditions, including MFP-I, thiolase, MTE-I, and CTE-I (data not shown).

We examined the expression of PPARα-regulated gene products in "Little" mice that carry a mutation in the *Ghrhr* gene. Compared with the Snell and Ames dwarf mice, the control *lit/lit* mice did not exhibit constitutive increases in any of the proteins examined (Fig. 4, B and C). However, the *lit/lit* mice exhibited increased expression of ACO-A, ACO-B, MFP-II thiolase, and MTE-1 proteins after WY-14,643 exposure compared with WY-14,643-treated +/*lit* mice, but only MFP-II attained statistical significance because of significant interactions between genotype and treatment for the other proteins (Fig. 4, B and C).

We examined fatty acid catabolism protein expression in the livers of control wild-type and GHR-null mice. Cyp4a and thiolase exhibited increased levels in untreated GHR-null mice compared with the untreated wild-type mice (Fig. 4D). Other fatty acid metabolism gene products were not appreciably altered in the GHR-null mice (data not shown). Taken together, these results indicate that in dwarf mice, expression of a subset of PPARα-regulated gene products is either constitutively up-regulated (Snell, Ames and GHR-null dwarf mice) or has increased responsiveness to a PP (Snell, Little dwarf mice), indicating that a growth hormone signaling pathway(s) plays a role in the regulation of several PPARα-dependent gene products.

Altered Expression in Dwarf Mice of PPARα-Regulated Gene Products Involved in Stress Resistance and Cardiovascular Disease. Based on the results of the transcript profiles, we examined the expression of gene products involved in protein folding and stress resistance that were increased by WY-14,643. The large family of proteins involved in protein folding including chaperones and chaperonin proteins [also called T-complex protein or chaperonin-containing T-complex protein-1, (CCT)] were initially examined. We were particularly interested in those proteins that we had previously demonstrated to be altered by PP exposure in a PPARα-dependent manner, including Hsp86, Hsp70, and T-complex protein-1 subunits (Anderson et al., 2004). We examined the expression of these proteins in the livers of control and WY-14,643-treated +/*dw* and *dw/dw* mice. Although Hsp86 and Hsp70 proteins exhibited increased levels after WY-14,643 exposure, there were no detectable differences in expression between the strains (data not shown). The results are consistent with lack of changes in *Hsp86* mRNA in *dw/dw* mice but do not reflect the increases in *Hsp70* mRNA, indicating that additional mechanisms control protein expression. We examined expression of T-complex protein 1 family members to which antibodies were available (T-complex

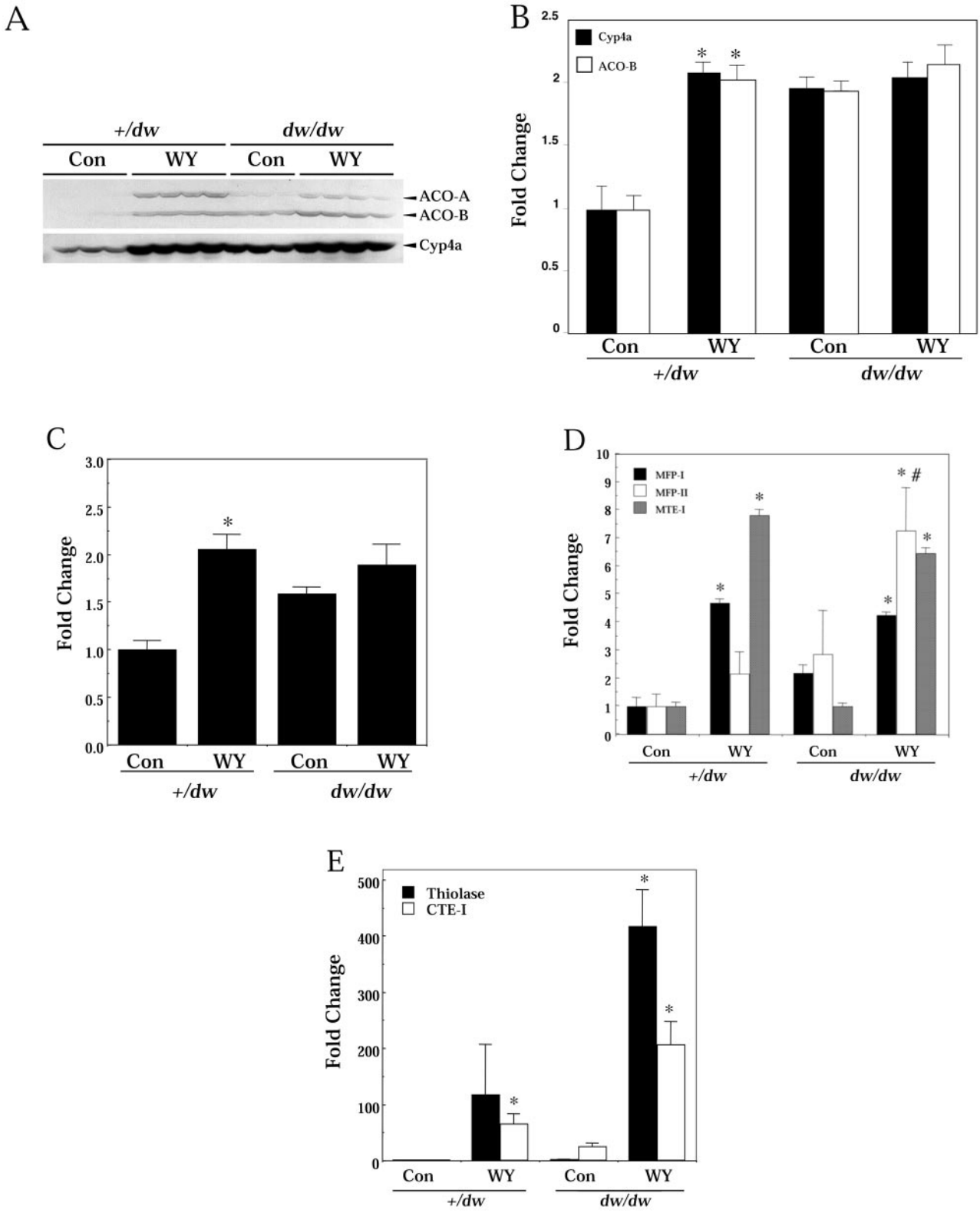

Fig. 2. Constitutive expression of PPARα-regulated gene products in Snell dwarf mice. *dw/dw* and *+/dw* mice were administered three consecutive gavage doses of WY-14,643 (50 mg/kg) in methylcellulose or methylcellulose alone and sacrificed after 72 h. A, Western blots showing ACO and Cyp4a expression. B, quantitation of Western blots in A. C, Palmitoyl-CoA oxidase activity. D and E, expression of other gene products under control of PPARα. Expression of multifunctional protein-I (MFP-I), multifunctional protein-II (MFP-II), thiolase, mitochondrial thioesterase-I (MTE-I), and cytosolic thioesterase-I (CTE-I) were determined by Western analyses using the same extracts described in A and quantified as in B. Error bars are means ± S.E. (n = 3–4/group). *, significant difference between the WY-14,643-treated and control group for each strain ($p < 0.05$). #, significant difference between the *dw/dw* and *+/dw* groups ($p < 0.05$).

protein-1α, -β, -ϵ). The increase in T-complex protein-1ϵ expression in the livers of wild-type SV129 mice was shown to be PPARα-dependent in that T-complex protein-1ϵ was increased in wild-type but not PPARα-null mice after WY-14,643 exposure (Fig. 5A). T-complex protein-1ϵ was increased in the control *dw/dw* strain but not the *lit/lit* strain compared with their respective heterozygote control mice (Fig. 5B). These results are consistent with the RT-PCR results showing a modest induction of the *Cct5* gene. T-complex protein-1ϵ expression was significantly increased after WY-14,643 treatment in both *dw/dw* and *lit/lit* dwarf strains as well as heterozygote strains (Fig. 5B). It is surprising that the expression of the *Cct5* gene was not altered by WY-14,643 treatment in either strain. Like the fatty acid catabolism genes discussed above, T-complex protein-1ϵ was increased to a greater extent in WY-14,643-treated *dw/dw* mice compared with WY-14,643-treated +/*dw* mice (Fig. 5B). T-complex protein-1ϵ was also elevated in the livers of GHR-null mice compared with wild-type mice (Fig. 5C). No changes in the expression of other chaperones or chaperonins, including T-complex protein-1α, T-complex protein-1β, ERp72, Hsp25, Hsp60, Hsp65, and Hsp84 were noted in the livers or hearts from control and WY-14,643-treated Snell dwarf mice or in the livers from GHR-null mice (data not shown).

We performed a preliminary examination of PPARα-regulated gene products in the kidneys of Snell dwarf mice from the same 3-day WY-14,643 study described above. Like the

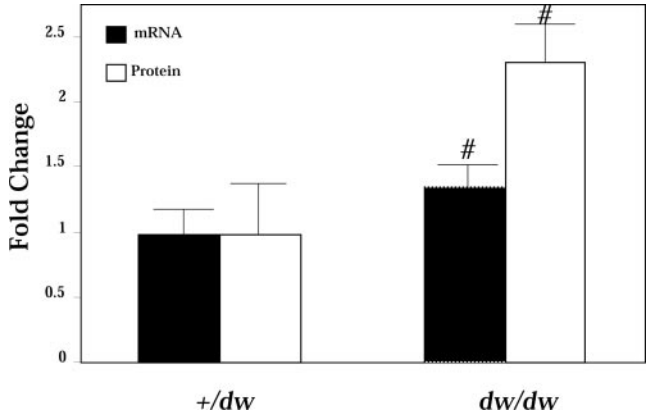

Fig. 3. Increased expression of PPARα in the livers of Snell dwarf mice. Expression of PPARα mRNA and protein were determined in the mouse livers described in Fig. 2. Error bars are means ± S.E. (n = 3–4/group). #, significant difference between the control *dw/dw* and +/*dw* groups ($p < 0.05$).

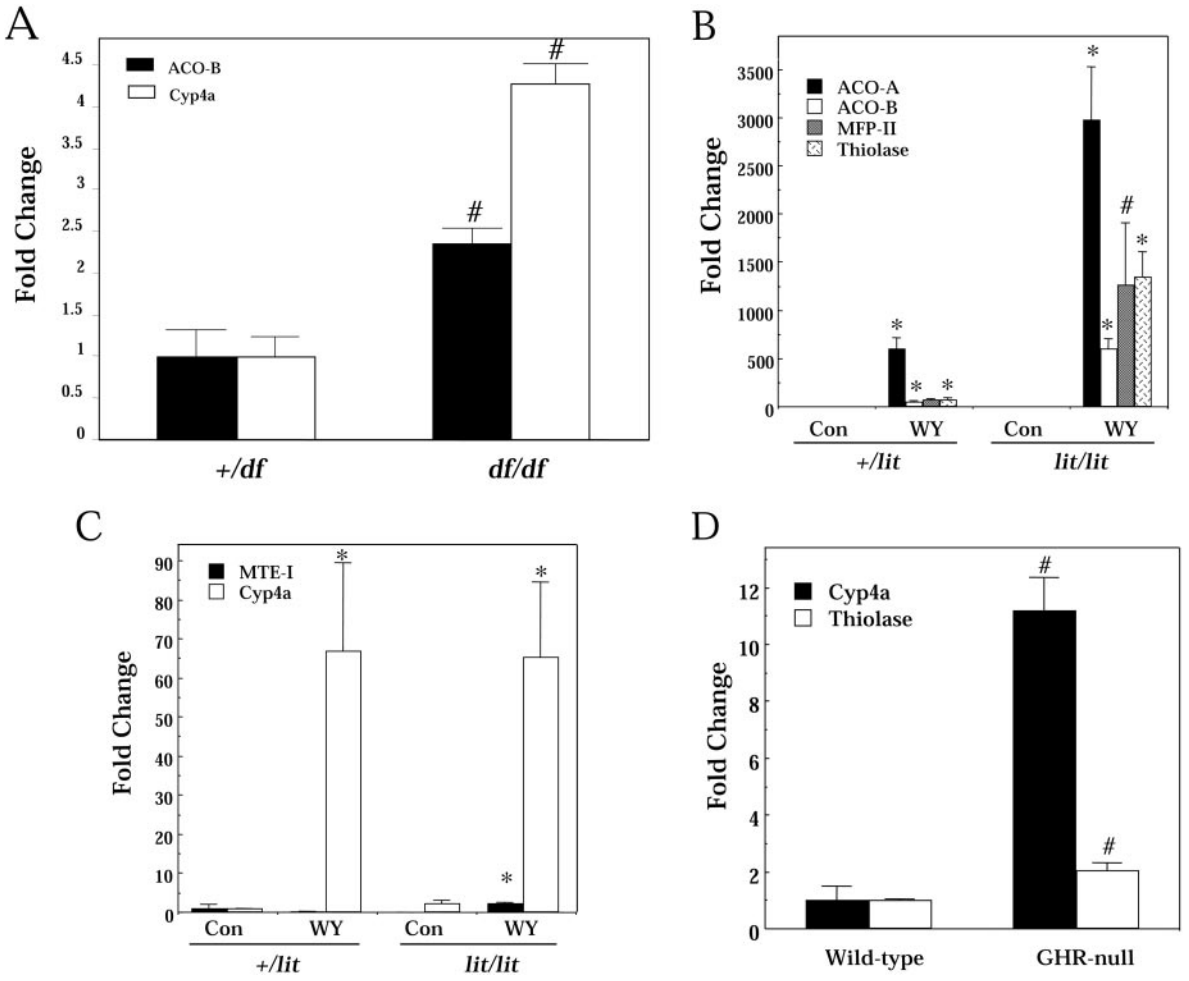

Fig. 4. Expression of PPARα-regulated lipid metabolizing enzymes in dwarf mice. A, expression of ACO-B and Cyp4a proteins in the livers of control heterozygote (+/*df*) and Ames dwarf (*df/df*) mice. B and C, expression of PPARα-regulated gene products in control or WY-14,643-treated heterozygote (+/*lit*) or Little dwarf (*lit/lit*) mice. Mice were administered three consecutive gavage doses of WY-14,643 (50 mg/kg) in methylcellulose or methylcellulose alone and sacrificed after 72 h. D, expression of thiolase and Cyp4a determined in the livers of control wild-type and GHR-null mice. Error bars are means ± S.E. (n = 3–4/group). *, significant difference between the WY-14,643-treated and control group ($p < 0.05$). #, significant difference between the dwarf and wild-type groups ($p < 0.05$).

liver, Cyp4a protein levels were elevated in the kidneys of WY-14,643-treated +/*dw* and *dw*/*dw* mice (Fig. 5D). T-complex protein-1ϵ exhibited increased expression in WY-14,643-treated +/*dw* mice compared with control +/dw mice (Fig. 5E). The expression of the chaperone Hsp25 was also increased in control *dw*/*dw* mice compared with control +/*dw* mice but not after WY-14,643-treatment in either strain (Fig. 5E). No changes in the expression of T-complex protein-1α, T-complex protein-1β, ERp72, Hsp60, Hsp65, and Hsp84 were noted in the kidneys from control and WY-14,643-treated Snell dwarf mice (data not shown). These results indicate that the chaperonin T-complex protein-1ϵ and Hsp25 are constitutively elevated in the kidneys of Snell dwarf mice.

PPARα regulates a large battery of genes expressed in the liver whose gene products play roles in atherosclerosis through lipid transport, inflammation, and clot formation. A number of these genes encode acute phase proteins (APP) that are elevated during times of acute or chronic infection. PP generally down-regulate the expression of these APP, possibly through the negative regulation by PPARα of transcription factors controlling APP gene expression (Corton et al., 2000). Given that the transcript profiling results predicted a general decrease in inflammatory responses in control *dw*/*dw* and WY-14,643-treated +/*dw* mice through decreases in receptors for interleukin 1 and interferon gamma, we examined the expression of APP in the livers of dwarf mice known to be regulated by WY-14,643 (Corton et al., 1998). All fibrinogen subunits (α, β, and γ) were down-regulated in control *dw*/*dw* compared with control +/*dw* mice, although decreases in α- and β-fibrinogen did not reach statistical significance (Fig. 6A). Under these

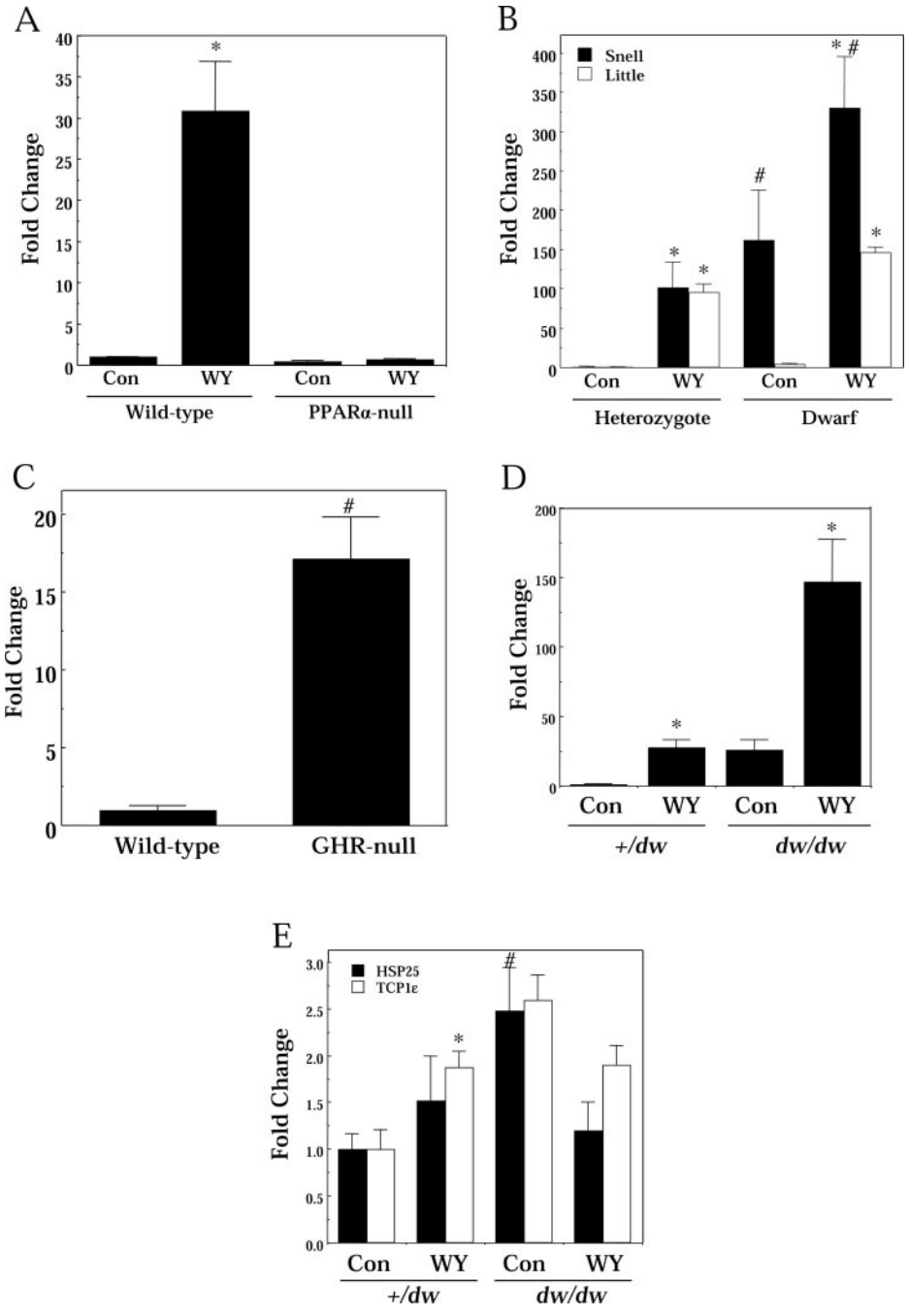

Fig. 5. Altered expression of a PPARα-regulated chaperonin in dwarf mice. A, WY-14,643 induction of T-complex protein-1ϵ is PPARα-dependent. Wild-type and PPARα-null mice were treated with WY-14,643 in the diet for 7 days. Liver homogenates were used to determine expression of T-complex protein-1ϵ by Western analysis. B, T-complex protein-1ϵ expression in dwarf mouse livers. T-complex protein-1ϵ protein expression was assessed by Western blot in the livers of WY-14,643- and control-treated *dw*/*dw* (Snell) and +/*dw* mice and *lit*/*lit* (Little) and +/*lit* mice described in Figs. 2 and 4, respectively. C, T-complex protein-1ϵ expression in GHR-null mouse livers. D, expression of Cyp4a in the kidneys of *dw*/*dw* and +/*dw* mice. E, expression of T-complex protein-1ϵ and Hsp25 in the kidneys of *dw*/*dw* and +/*dw* mice. T-complex protein-1ϵ and Hsp25 protein expression was assessed by Western blot in the kidneys of WY-14,643- and control-treated +/*dw* and *dw*/*dw* mice described in Fig. 2. Error bars are means ± S.E. (n = 3–4/group). *, significant difference between the WY-14,643-treated and control groups ($p < 0.05$). #, significant difference between the dwarf and wild-type groups ($p < 0.05$).

conditions WY-14,643 had no significant effect on fibrinogen levels in +/*dw* mice. Longer exposure times may be required to decrease fibrinogen gene and protein levels (Corton et al., 1998) and would explain why α-fibrinogen, a gene on the Atlas Cancer 1.2 array, was not identified as down-regulated 12 h after WY-14,643 exposure. There was a significant decrease in the expression of α- and γ-fibrinogen in WY-14,643-treated *dw*/*dw* mice compared with WY-14,643-treated +/*dw* mice. Another APP gene product, α_1-antitrypsin, exhibited decreased expression in WY-14,643-treated +/dw compared with control +/dw mice (Fig. 6A). Decreased levels of α_1-anti-trypsin in control and WY-14,643-treated *dw*/*dw* mice were not comparable with +/dw mice because of a significant interaction. β-Fibrinogen levels exhibited decreases by WY-14,643 in both +/*lit* and *lit*/*lit* strains (Fig. 6B). Although levels of β-fibrinogen were decreased in the control *lit*/*lit* compared with the control +/*lit* strain, a significant interaction between genotype and treatment prevented statistical comparison. Finally, GHR-null mice had decreased levels of β-fibrinogen compared with wild-type control mice (Fig. 6C). These results indicate that some markers of inflammation and atherosclerosis are decreased in dwarf mice in a manner similar to PP exposure in wild-type mice.

Discussion

We posed the hypothesis that the overlap in the phenotypic effects of PP treatment in wild-type mice and control dwarf mice has as its basis an overlap in the transcriptional programs regulated by PPARα. We examined gene expression by transcript profiling in the livers of Snell (*Pit-1*^{dw}) dwarf (*dw*/*dw*) and heterozygote (+/*dw*) mice treated with WY-14,643. Control *dw*/*dw* mice exhibited characteristics of PPARα activation. Of the 41 genes identified as differentially regulated in control *dw*/*dw* mice versus control +/*dw* mice, 41% were regulated similarly by WY-14,643 in +/*dw* mice. Many PPARα target genes and their protein products involved in fatty acid metabolism were increased in control Snell dwarf livers. The increase in PPARα-regulated gene products involved in lipid metabolism was found to various extents in the livers of three additional dwarf mouse models that have in common defects in growth hormone secretion and/or signaling. Ames dwarf mice exhibited increased expression of ACO and Cyp4a, whereas GHR-null mice exhibited increases in thiolase and Cyp4a. Little and Snell mice exhibited greater inductions of lipid metabolism gene products after WY-14,643 exposure compared with corresponding WY-14,643-treated heterozygote strains, demonstrating greater responsiveness to PP in these dwarf mice. The increases in lipid metabolism genes may be caused by increases in PPARα mRNA and protein as observed in the livers of control *dw*/*dw* mice. These results are consistent with two studies that showed an inverse relationship between growth hormone signaling and PPARα-regulated gene expression. Mice with defects in growth hormone-responsive STAT5b transcription

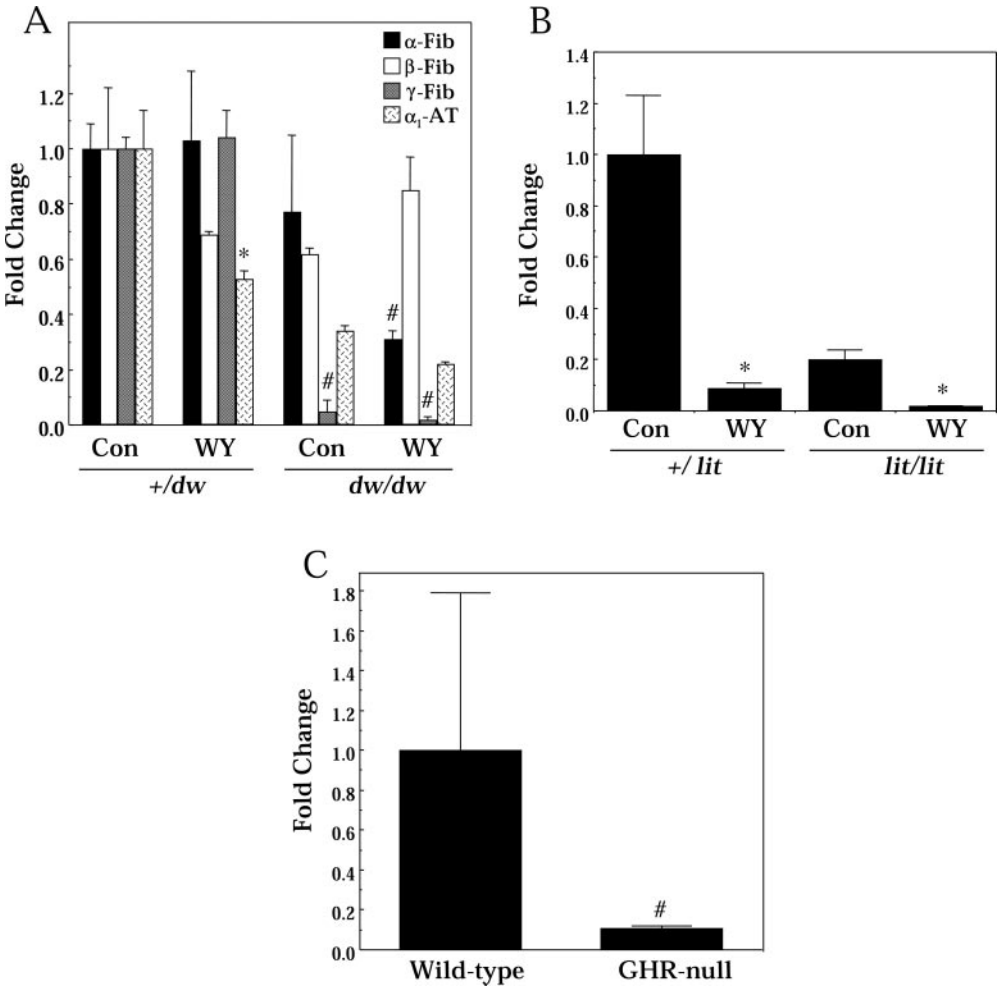

Fig. 6. Altered expression in dwarf mice of PPARα-regulated gene products involved in cardiovascular disease. A, expression of fibrinogen (Fib) and α_1-antitrypsin (α_1-AT) in the livers of +/*dw* and *dw*/*dw* mice. Expression was determined by Western analyses in the livers of mice described in Fig. 2. B, expression of β-fibrinogen in the livers of Little dwarf mice. Expression was determined by Western analyses in the livers of mice described in Fig. 4. C, expression of β-fibrinogen in the livers of wild-type and GHR-null mice. Expression of β-fibrinogen was determined in the livers of mice described in Fig. 4. Error bars are means ± S.E. (n = 3–4/group). *, significant difference between the WY-14,643-treated and control groups ($p < 0.05$). #, significant difference between the control dwarf and wild-type groups ($p < 0.05$).

factor also exhibited constitutive increases in PPARα-regulated gene expression (Zhou et al., 2002). On the other hand, a transcript profiling study in the livers of growth hormone-treated rats revealed a subset of PPARα-regulated genes that were down-regulated, including *CYP4A3* as well as *PPARα* itself (Tollet-Egnell et al., 2001). Taken together, mice with defects in growth hormone secretion and signaling exhibit increased constitutive expression of a subset of lipid metabolizing gene products under control of PPARα.

In addition to the lipid metabolism genes identified here, WY-14,643 and dwarf mutations alter additional gene products with links to cardiovascular disease. Fibrinogen and α_1-anti-trypsin are acute phase proteins that are used as general indicators of inflammatory processes associated with atherogenesis (Barbier et al., 2002). An elevated plasma fibrinogen level is an independent risk factor for coronary heart disease, stroke, and peripheral vascular disease. APP genes are negatively regulated by PP in a PPARα-dependent manner (Corton et al., 1998, 2000). At least one of the fibrinogen family members was down-regulated in two dwarf mouse models (Snell, GHR-null). α_1-Anti-trypsin was down-regulated in Snell mice. The basis for the down-regulation of the APP by PP may be the ability of PPARα to negatively interfere with the actions of the transcription factors nuclear factor-κB, activator protein-1, nuclear factor of activated T cells, and CCAAT/enhancer-binding protein β, which regulate pro-inflammatory genes (Barbier et al., 2002). Because PPARα is a common regulator of factors that impact atherosclerosis (Barbier et al., 2002), the induction of PPARα and regulated genes in dwarf mice may lead to decreases in not only circulating triglyceride and cholesterol levels (H. Brown-Borg, unpublished observations) through modulation of lipid metabolism genes but also negative regulation of inflammatory genes that contribute to cardiovascular disease.

The chaperonin family of related T-complex protein-1 proteins interact with hydrophobic regions on nascent polypeptide chains, preventing aggregation and subsequent toxicity. Like the chaperone heat shock proteins, the chaperonins are induced after physical or chemical stress in which protein denaturation is a prominent feature (Yokota et al., 2000). Low-level exposure to different stressors leads to increased expression of chaperonins and chaperones that better protect the cell from further insults (Latchman, 2001). We found that the T-complex protein-1ϵ protein was induced by both WY-14,643 and dwarf mutations. Increased expression was found in the livers of Snell and GHR-null mice. The T-complex protein-1 gene (*Cct5*) was also induced in control *dw/dw* mice but not by WY-14,643 in either strain. Although additional genes involved in protein folding were induced in control *dw/dw* mice including *Cct3*, *Hsp60*, and *Hsp70*, other genes were not, indicating that the dwarf mutations do not lead to a general increase in the expression of the protein-folding machinery. The livers of PP-treated wild-type mice in which many heat-shock proteins and T-complex protein-1ϵ are induced are protected from different types of chemical insults (Mehendale, 2000), including oxidative stress (Anderson et al., 2004). The relationship between the expression of T-complex protein-1ϵ and increased protection of Snell fibroblasts to different forms of stress (Murakami et al., 2003) needs to be examined.

The basis of the constitutive activation of PPARα and PPARα-regulated gene products in dwarf mice may be the abolishment of growth hormone-responsive STAT5b interference with PPARα activity. The ability of STAT5b to negatively regulate PPARα required the ligand-independent activation function (AF-1) in the N terminus of PPARα but not the C-terminal ligand-dependent AF-2 (Zhou and Waxman, 1999a,b). These activation functions probably recognize overlapping sets of interacting coactivators and corepressors, resulting in regulation of distinct sets of genes. Negative interference of PPARα by STAT5b could occur by a number of mechanisms, including 1) interference with the ability of PPARα to bind a PPRE or interact with appropriate coactivators/corepressors or 2) competition for essential coactivators or other interacting proteins (Zhou and Waxman, 1999a,b). In our study, not all PP-dependent gene products were constitutively regulated by *pit-1*^{dw} but required WY-14,643 exposure for induction in dwarf mice. Differences in *pit-1* dependent (e.g., *Acox1*, *Cyp4a10*, *Cyp4a14)* and WY-14,643-dependent (e.g., *Mte1*) induction in Snell dwarf mice may reflect differences in the requirement for AF-1 versus AF-2 for gene activation. Only those genes that require the STAT5b-inhibitable AF-1 would be *pit-1* dependent. Exposure of dwarf mice to WY-14,643 did not further increase the expression of some *pit-1*-dependent gene products (e.g., *Fabp4*), possibly because of the high intrinsic activity of AF-1 compared with AF-2.

In addition to the interference of PPARα activity by STAT5b, PPARα can negatively interfere with the ability of STAT5b to activate growth hormone-responsive genes. The AF-1 of PPARα was required for negative interference of STAT5b, but how PPARα interferes with STAT5b function is not known (Shipley and Waxman, 2003). These studies imply that given the correct cellular context in which PPARα and STAT5b are both expressed, PP could act as dwarf mouse mimetics through inhibition of STAT5b. Thus, it may be possible not only that some of the beneficial effects of the dwarf genotype occur through activation of PPARα but also that activation of PPARα by PP in wild-type animals may negatively interfere with growth hormone signaling and lead to dwarf mouse-like effects. PP exposure leads to changes similar to those caused by defects in growth hormone signaling, including increases in the fatty acid-metabolizing genes identified here as well as down-regulation of growth hormone-regulated cytochrome P450 family members (Corton et al., 1998). Compounds that mimic the dwarf mouse phenotype would ideally target the PPARα AF-1. With this in mind, mitogen-activated protein kinase activates PPARα through the AF-1 activation domain important for insulin-dependent signaling (Juge-Aubry et al., 1999) and cardiac metabolic stress responses (Barger et al., 2001).

PPARα may play roles in other models of stress resistance and/or longevity. Using comprehensive transcript profiling, PPARα was required for ~20% of the gene expression changes in the liver after a 5-week caloric restriction (CR) and is required for CR to protect the liver from a lethal dose of thioacetamide, a hepatotoxic agent (Corton et al., 2004). As in the livers of Snell dwarf mice, the PPARα-dependent CR genes included those involved in fatty acid metabolism (i.e., *Cyp4a10*, *Cyp4a14*). With our findings of increased expression of PPARα-dependent genes in dwarf mice, alterations in PPARα target gene regulation seems to be common in many animal models of longevity and/or stress resistance. A dwarf mouse strain in which the PPARα gene is inactivated will be

important to unequivocally establish PPARα's role in the beneficial effects associated with defects in growth hormone signaling.

Acknowledgments

We thank Dr. Andrzej Bartke for tissues, Dennis House for assistance in performing some of the statistics, the CIIT Animal Care and Necropsy and Histology Units for assistance in performing these studies, Drs. Alexson and Hashimoto for antibodies, Drs. Igor Dozmorov and Richard Miller for providing the list of genes regulated in dwarf mice, Sharlene Rakoczy for technical assistance, and Drs. Kevin Gaido and Rusty Thomas for critical review of the manuscript.

References

Anderson SP, Howroyd P, Liu J, Qian X, Bahnemann R, Swanson C, Kwak MK, Kensler TW, and Corton JC (2004) The transcriptional response to a peroxisome proliferator-activated receptor α agonist includes increased expression of proteome maintenance genes. *J Biol Chem* **279:**52390–52398.

Anderson SP, Yoon L, Richard EB, Dunn CS, Cattley RC, and Corton JC (2002) Delayed liver regeneration in peroxisome proliferator-activated receptor-alpha-null mice. *Hepatology* **36:**544–554.

Barbier O, Torra IP, Duguay Y, Blanquart C, Fruchart JC, Glineur C, and Staels B (2002) Pleiotropic actions of peroxisome proliferator-activated receptors in lipid metabolism and atherosclerosis. *Arterioscler Thromb Vasc Biol* **22:**717–726.

Barger PM, Browning AC, Garner AN, and Kelly DP (2001) p38 mitogen-activated protein kinase activates peroxisome proliferator-activated receptor α: a potential role in the cardiac metabolic stress response. *J Biol Chem* **276:**44495–44501.

Bielschowsky F and Bielschowsky M (1961) Carcinogenesis in the pituitary of dwarf mouse. The response to dimethylbenzanthracene applied to the skin. *Br J Cancer* **15:**257–262.

Borg KE, Brown-Borg HM, and Bartke A (1995) Assessment of the primary adrenal cortical and pancreatic hormone basal levels in relation to plasma glucose and age in the unstressed Ames dwarf mouse. *Proc Soc Exp Biol Med* **210:**126–133.

Brown-Borg HM and Rakoczy SG (2000) Catalase expression in delayed and premature aging mouse models. *Exp Gerontol* **35:**199–212.

Bugni JM, Poole TM, and Drinkwater NR (2001) The little mutation suppresses DEN-induced hepatocarcinogenesis in mice and abrogates genetic and hormonal modulation of susceptibility. *Carcinogenesis* **22:**1853–1862.

Cattley RC and Popp JA (1989) Differences between the promoting activities of the peroxisome proliferator WY-14,643 and phenobarbital in rat liver. *Cancer Res* **49:**3246–3251.

Conway JG, Tomaszewski KE, Olson MJ, Cattley RC, Marsman DS, and Popp JA (1989) Relationship of oxidative damage to the hepatocarcinogenicity of the peroxisome proliferators di(2-ethylhexyl)phthalate and Wy-14,643. *Carcinogenesis* **10:**513–519.

Corton JC, Fan LQ, Brown S, Anderson SP, Bocos C, Cattley RC, Mode A, and Gustafsson JA (1998) Down-regulation of cytochrome P450 2C family members and positive acute-phase response gene expression by peroxisome proliferator chemicals. *Mol Pharmacol* **54:**463–473.

Corton JC, Anderson SP, and Stauber A (2000) Central role of peroxisome proliferator-activated receptors in the actions of peroxisome proliferators. *Annu Rev Pharmacol Toxicol* **40:**491–518.

Corton JC, Apte U, Anderson SP, Limaye P, Yoon L, Latendresse J, Dunn C, Everitt JI, Voss KA, Swanson C, et al., (2004) Caloric restriction mimetics include agonists of lipid-activated nuclear receptors. *J Biol Chem* **279:**46204–46212.

Dozmorov I, Galecki A, Chang Y, Krzesicki R, Vergara M, and Miller RA. Gene expression profile of long-lived snell dwarf mice. *J Gerontol A Biol Sci Med Sci* **57:**B99–B1082.

Eisen MB, Spellman PT, Brown PO, and Botstein D (1998) Cluster analysis and display of genome-wide expression patterns. *Proc Natl Acad Sci USA* **95:**14863–14868.

Howroyd P, Swanson C, Dunn C, Cattley RC, and Corton JC (2004) Decreased longevity and enhancement of age-dependent lesion in mice lacking the nuclear receptor peroxisome proliferator-activated receptor α (PPARα) *Toxicol Pathol*, in press.

Ikeno Y, Bronson RT, Hubbard GB, Lee S, and Bartke A (2003) Delayed occurrence of fatal neoplastic diseases in Ames dwarf mice: correlation to extended longevity. *J Gerontol A Biol Sci Med Sci* **58:**291–296.

Juge-Aubry CE, Hammar E, Siegrist-Kaiser C, Pernin A, Takeshita A, Chin WW, Burger AG, and Meier CA (1999) Regulation of the transcriptional activity of the peroxisome proliferator-activated receptor α by phosphorylation of a ligand-independent trans-activating domain. *J Biol Chem* **274:**10505–10510.

Kepler TB, Crosby L, and Morgan KT (2002). Normalization and analysis of DNA microarray data by self-consistency and local regression. *Genome Biol* **3(7):** RESEARCH0037.

Klaunig JE, Babich MA, Baetcke KP, Cook JC, Corton JC, David RM, DeLuca JG, Lai DY, McKee RH, Peters JM, et al. (2003) PPARalpha agonist-induced rodent tumors: modes of action and human relevance. *Crit Rev Toxicol* **33:**655–780.

Latchman DS (2001) Heat shock proteins and cardiac protection. *Cardiovasc Res* **51:**637–646.

Lee SS, Pineau T, Drago J, Lee EJ, Owens JW, Kroetz DL, Fernandez-Salguero PM, Westphal H, and Gonzalez FJ (1995) Targeted disruption of the alpha isoform of the peroxisome proliferator-activated receptor gene in mice results in abolishment of the pleiotropic effects of peroxisome proliferators. *Mol Cell Biol* **15:**3012–3022.

Liu PC, Huber R, Stow MD, Schlingmann KL, Collier P, Liao B, Link J, Burn TC, Hollis G, Young PR, et al. (2003) Induction of endogenous genes by peroxisome proliferator activated receptor alpha ligands in a human kidney cell line and in vivo. *J Steroid Biochem Mol Biol* **85:**71–79.

Marmary Y, Parlow AF, Goldsmith CM, He X, Wellner RB, Satomura K, Kriete MF, Robey PG, Nieman LK, and Baum BJ (1999) Construction and in vivo efficacy of a replication-deficient recombinant adenovirus encoding murine growth hormone. *Endocrinology* **140:**260–265.

Mehendale HM (2000) PPAR-alpha: a key to the mechanism of hepatoprotection by clofibrate. *Toxicol Sci* **57:**187–190.

Murakami S, Salmon A and Miller RA (2003) Multiplex stress resistance in cells from long-lived dwarf mice. *FASEB J* **17:**1565–1566.

Rennels EG, Anigstein DM, and Anigstein L (1965) A cumulative study of the growth of sarcoma 180 in anterior pituitary dwarf mice. *Tex Rep Biol Med* **23:**776–781.

Sausen PJ, Lee DC, Rose ML, and Cattley RC (1995) Elevated 8-hydroxydeoxyguanosine in hepatic DNA of rats following exposure to peroxisome proliferators: relationship to mitochondrial alterations. *Carcinogenesis* **16:**1795–1801.

Shipley JM and Waxman DJ (2003) Down-regulation of STAT5b transcriptional activity by ligand-activated peroxisome proliferator-activated receptor (PPAR) α and PPARγ. *Mol Pharmacol* **64:**355–364.

Sterchele PF, Sun H, Peterson RE, and Vanden Heuvel JP (1996) Regulation of peroxisome proliferator-activated receptor-alpha mRNA in rat liver. *Arch Biochem Biophys* **326:**281–289.

Styles JA, Kelly MD, Pritchard NR, and Foster JR (1990) Effects produced by the non-genotoxic hepatocarcinogen methylclofenapate in dwarf mice: peroxisome induction uncoupled from DNA synthesis and nuclearity changes. *Carcinogenesis* **11:**387–391.

Sugiyama H, Yamada J, and Suga T (1994) Effects of testosterone, hypophysectomy and growth hormone treatment on clofibrate induction of peroxisomal beta-oxidation in female rat liver. *Biochem Pharmacol* **47:**918–921.

Tatar M, Bartke A, and Antebi A (2003) The endocrine regulation of aging by insulin-like signals. *Science (Wash DC)* **299:**1346–1351.

Thuillier P, Anchiraico GJ, Nickel KP, Maldve RE, Gimenez-Conti I, Muga SJ, Liu KL, Fischer SM, and Belury MA (2000) Activators of peroxisome proliferator-activated receptor-alpha partially inhibit mouse skin tumor promotion. *Mol Carcinog* **29:**134–142.

Tollet-Egnell P, Flores-Morales A, Stahlberg N, Malek RL, Lee N, and Norstedt G (2001) Gene expression profile of the aging process in rat liver: normalizing effects of growth hormone replacement. *Mol Endocrinol* **15:**308–318.

Yokota SI, Yanagi H, Yura T, and Kubota H (2000) Cytosolic chaperonin-containing t-complex polypeptide 1 changes the content of a particular subunit species concomitant with substrate binding and folding activities during the cell cycle. *Eur J Biochem* **267:**1658–1664.

Zhou Y, Xu BC, Maheshwari HG, He L, Reed M, Lozykowski M, Okada S, Cataldo L, Coschigamo K, Wagner TE, Baumann G and Kopchick JJ (1997) A mammalian model for Laron syndrome produced by targeted disruption of the mouse growth hormone receptor/binding protein gene (the Laron mouse). *Proc Natl Acad Sci USA* **94:**3215–3220.

Zhou YC, Davey HW, McLachlan MJ, Xie T, and Waxman DJ (2002) Elevated basal expression of liver peroxisomal beta-oxidation enzymes and CYP4A microsomal fatty acid omega-hydroxylase in STAT5b(−/−) mice: cross-talk in vivo between peroxisome proliferator-activated receptor and signal transducer and activator of transcription signaling pathways. *Toxicol Appl Pharmacol* **182:**1–10.

Zhou YC and Waxman DJ (1999a) Cross-talk between janus kinase-signal transducer and activator of transcription (JAK-STAT) and peroxisome proliferator-activated receptor-α (PPARα) signaling pathways. Growth hormone inhibition of pparalpha transcriptional activity mediated by stat5b. *J Biol Chem* **274:**2672–2681.

Zhou YC and Waxman DJ (1999b) STAT5b down-regulates peroxisome proliferator-activated receptor α transcription by inhibition of ligand-independent activation function region-1 trans-activation domain. *J Biol Chem* **274:**29874–29882.

Address correspondence to: J. Christopher Corton, ToxicoGenomics, 209 Silver Creek Tr., Chapel Hill, NC 27514. E-mail: ccorton@msn.com